High-power diode-pumped Yb-doped fiber laser at 1150 nm

Yu Miao (苗 宇), Hanwei Zhang (张汉伟), Hu Xiao (肖 虎)*, and Pu Zhou (周 朴)**

College of OptoElectric Science and Engineering, National University of Defense Technology, Changsha 410073, China

**Corresponding author: xhwise@gmail.com; ***corresponding author: zhoupu203@163.com*

Received April 7, 2014; accepted June 11, 2014; posted online August 27, 2014

A model of steady-state rate equations including amplified spontaneous emission for long-wavelength Yb doped fiber laser is set up, which provides design principle for a practical laser system. We demonstrate a diode-pumped all-fiber Yb-doped fiber laser at 1150 nm with an output power of 33.6 W, the optical efficiency is 60%.

OCIS codes: 140.3510, 060.3510.
doi: 10.3788/COL201412.091403.

Over the past decade, Yb-doped fiber lasers (YDFLs) are well developed due to their outstanding characteristics, such as high efficiency, good beam quality, and convenient thermal management[1,2]. The oscillation spectral range of YDFLs can be divided into three bands, namely, convenient (C-band, 1060–1130 nm), short (S-band, 976–980 and 1020−1060 nm), and long (L-band, > 1130 nm) bands[3]. Most of the previous literature studies focus on C-band YDFLs. Actually, L-band YDFLs also have many special applications. For example, YDFLs in the range of 1120–1160 nm can be used as pump sources for Ho-Tm-doped fiber lasers in mid-infrared region[4–10]. Besides, YDFLs in the range of 1150–1180 nm can be transferred to yellow light through frequency doubling, which is a good source for applications in medicine and astronomy[11–13]. Due to the requirement of above-mentioned applications, L-band YDFLs have achieved extensive attention in recent years. In 2006, Kurkov *et al.* realized a YDFL emitting at 1160 nm with a maximum output power of 3.2 W[14]. In 2008, Dvoyrin *et al.* achieved a fiber laser at 1160 nm by tandem pump with another YDFL emitting at 1070 nm, a maximum output power of 9.1 W with a slope efficiency of about 25–30% was obtained[15]. In 2009, diode-pumped linearly polarized YDFL with a maximum output power of 18 W at 1154 nm was reported[16]. In 2013, diode-pumped YDFL operating at 1160 nm with 21 W output power and YDFL at 1147 nm with a maximum output power of 35 W were reported[17]. As indicated by Kurkov *et al.*[7], Ho^{3+}-ions have a absorbance peak in the 1150 nm range, thus, high-power YDFLs at 1150 nm can be a good source for high-power mid-infrared fiber laser.

We report a diode-pumped YDFL emitting at 1150 nm. Specific attention is paid to amplified spontaneous emission (ASE) and parasitic lasing effect in the 1070 nm range. A theoretical model is presented to optimize the parameters in the experiment. YDFL at 1150 nm with an output power of 33.6 W and an optical efficiency of 60% is demonstrated.

Here we set up a theoretical model including ASE. Based on this model, we theoretically study the relationship between ASE and output power with the reflectivity of output coupler (OC) fiber Bragg grating (FBG) and the length of Yb-doped fiber (YDF). The model can be expressed by steady-state rate equations[18,19].

$$\frac{N_2(z)}{N}=\frac{\dfrac{P_p^{\pm}(z)\sigma_a(\lambda_p)\Gamma_p}{h\nu_p A}+\sum_k\dfrac{P^{\pm}(z,\lambda_k)\sigma_a(\lambda_k)\Gamma_k}{h\nu_k A}}{\dfrac{P_p^{\pm}(z)[\sigma_a(\lambda_p)+\sigma_e(\lambda_p)]\Gamma_p}{h\nu_p A}+\dfrac{1}{\tau}+\sum_k\dfrac{P^{\pm}(z,\lambda_k)[\sigma_a(\lambda_k)+\sigma_e(\lambda_k)]\Gamma_k}{h\nu_k A}}, \tag{1}$$

$$\pm\frac{\mathrm{d}P_p^{\pm}(z)}{\mathrm{d}z}=-\Gamma_p\{\sigma_a(\lambda_p)N-[\sigma_a(\lambda_p)+\sigma_e(\lambda_p)]\,N_2(z)\}P_p^{\pm}(z)-\alpha(\lambda_p)P_p^{\pm}(z), \tag{2}$$

$$\pm\frac{\mathrm{d}P^{\pm}(z,\lambda_k)}{\mathrm{d}z}=-\Gamma_s\{[\sigma_a(\lambda_k)+\sigma_e(\lambda_k)]N_2(z)-\sigma_a(\lambda_k)N\}P^{\pm}(z,\lambda_k)+2\Gamma_s\sigma_e(\lambda_k)N_2(z)\frac{hc^2}{\lambda_k^3}\Delta\lambda-\alpha(\lambda_k)P^{\pm}(z,\lambda_k), \tag{3}$$

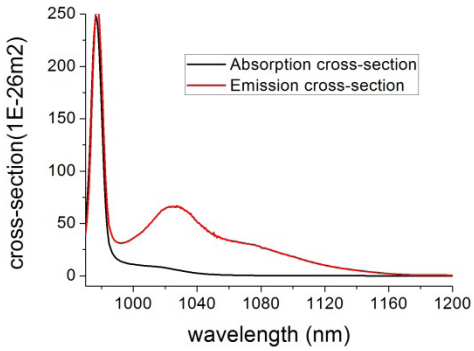

Fig. 1. Absorption and emission cross-section values of YDF.

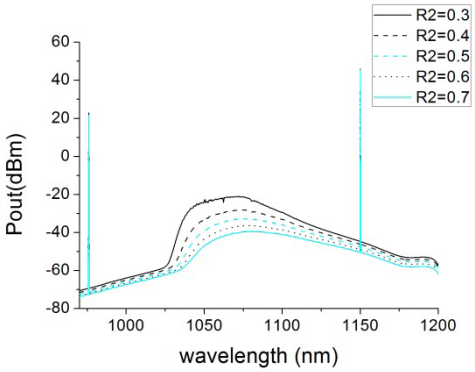

Fig. 2. Laser output spectrum with different reflectivities of FBG.

where N_2 is the concentration of the ions in the excited state, P_p is the pump power, z is the axial coordinate in the gain fiber, $P(z, \lambda_k)$ is the power of ASE at λ_k, A is the area of the core, τ is the lifetime of gain medium, Γ_p, Γ_k, and Γ_s are the fill factors of pump light, ASE, and signal light, respectively, ν_p, λ_p, ν_k, and λ_k, are the frequencies and wavelengths of pump light and ASE; σ_a and σ_e are the absorption and emission cross-section, α is the intrinsic absorption coefficient, and the superscripts "+" and "−" mean forward and backward directions.

The boundary conditions are

$$P^+(0,\lambda_k) = R_1(\lambda_k)P^-(0,\lambda_k), \tag{4}$$

$$P^-(L,\lambda_k) = R_2(\lambda_k)P^+(L,\lambda_k), \tag{5}$$

where R_1 and R_2 are the reflectivities of signal light and ASE in the laser, which may come from sideband reflection of FBGs, reflection of fiber facet, and Rayleigh scattering.

In order to simplify calculation, we do not take the influence of spectral width of pump light to absorption into account and we assume that the reflectivity of ASE is not related to wavelength. The calculation is based on forward pumping. The parameters for numerical calculation are listed in Table 1, and the absorption and emission cross-section values are shown in Fig. 1[20]. It should be mentioned that the reflectivities for out-of-band wavelengths of R_1 and R_2 are 0.003, because wavelength-selective end reflectors can suppress 50 dB before the occurrence spurious lasing[21].

The relation between ASE and the reflectivity of OC FBG is shown in Fig. 2. We can find that high reflectivity (HR) of OC FBG has more potential to suppress ASE, and the parasitic lasing appears when the reflectivity is less than 0.3. Since the reflectivity increases, the density of signal light in the cavity increases at the same time, which can suppress ASE.

However, the output power decreases when we increase the reflectivity, which is shown in Fig. 3. Thus, in order to obtain high output power, we should choose OC FBG with a proper reflectivity.

The relation between ASE and the length of YDF is shown in Fig. 4. It shows that increasing the length of gain fiber has advantage for suppressing ASE to some extent, because if the gain fiber is longer, more light could be absorbed in the forward direction in the 1070 nm range. Although this has little impact on the backward ASE, the backward ASE will not be enhanced

Table 1. Main Parameters in the Simulation

Parameter	Value
N	$8 \times 10^{25}/\mathrm{m}^3$
τ	0.84 ms
NA	0.08
A	7.85×10^{-11} m^2
λ_p	976 nm
α_p	0.0025/m
α_s	0.0023/m
Γ_p	0.0064
Γ_s	0.8
R_1	0.99 ($\lambda = 1150$ nm) 0.003 ($\lambda \neq 1150$ nm)
R_2	0.003 ($\lambda \neq 1150$ nm)

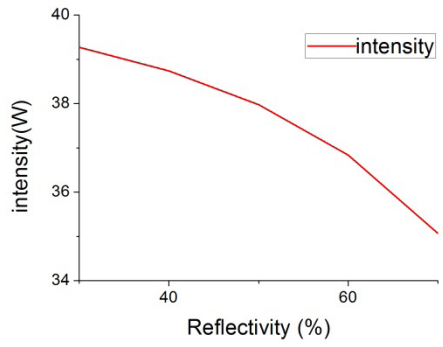

Fig. 3. Relation between output power and the reflectivity of OC FBG with 50 W pump power.

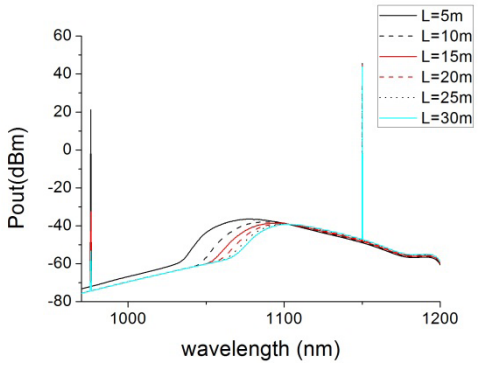

Fig. 4. Laser output spectrum with different lengths of YDF.

at least. However, the system cost will increase at the same time. Moreover, long gain fiber would also increase the background loss, which would be an important issue for our cavity[16].

The system setup is depicted in Fig. 5. It consists of a pump source, several meters of YDF, and a pair of FBGs. The pump source is two 976 nm laser diodes (LDs), whose maximal output power is 45 W. The central wavelength of the FBGs is 1150 nm and the reflectivity of HR FBG and OC FBG are 99% and 72%, respectively. The gain fiber is a 25 m long commercial double-clad YDF with core and inner cladding diameters of 10 and 125 μm. A combiner is employed to connect the LD and HR FBG. The output end is cleaved at an angle of 8° to avoid back reflection and parasitic oscillation. The whole system is under the room temperature of 22 °C.

The relation between output power and pump power is shown in Fig. 6. A maximum output power of 33.6 W is obtained with a pump power of 56 W, the optical efficiency is 60%.

The forward and backward spectra at maximal output power are shown in Figs. 7(a) and (b), which are measured by an optical spectrum analyzer (Yokogawa AQ6370C). The full-width at half-maximum (FWHM) bandwidth at maximal output power is 1.1 nm. It shows that there is no ASE at 1070 nm and the pump power was nearly totally absorbed in the forward spectrum, but ASE at 1070 nm is observed in the back spectrum. However, when we increase the pump power, the parasitic oscillation appears abruptly. The improvement of output power may be limited by the parasitic oscillation.

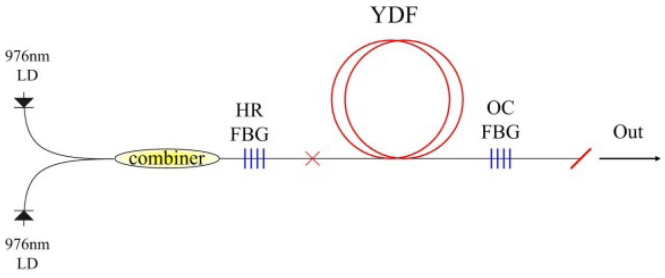

Fig. 5. Experimental setup of 1150 nm YDFL system.

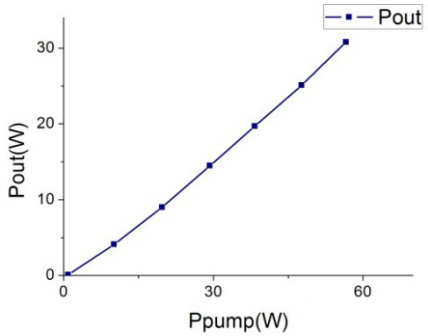

Fig. 6. Dependence of the output power of the 1150 nm laser on the 976 nm pump power.

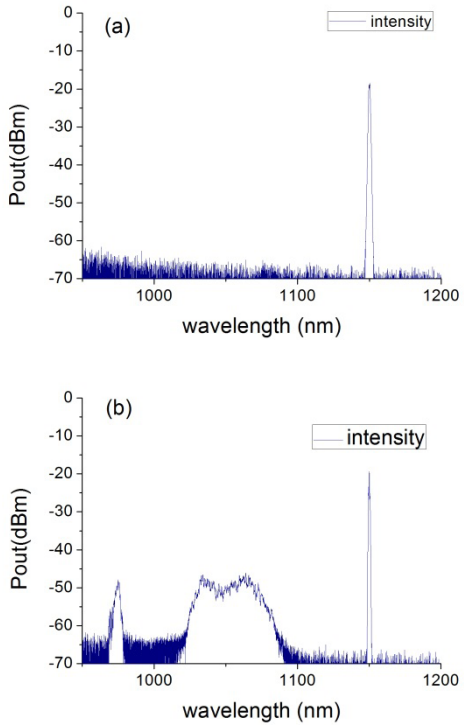

Fig. 7. (a) Forward spectrum at maximal output power of 1150 nm YDFL and (b) Back spectrum at maximal output power of 1150 nm YDFL.

In conclusion, we demonstrate an all-fiber YDFL at 1150 nm pumped by a LD. An output power of 33.6 W at 1150 nm is obtained with an optical efficiency of 60% and a FWHM bandwidth of 1.1 nm. Further power scaling may be limited by parasitic oscillation for the time being. Our next work will focus on methods to suppress parasitic oscillation.

References

1. D. J. Richardson, J. Nilsson, and W. A. Clarkson, J. Opt. Soc. Am. B **27,** B63 (2010).
2. H. Xiao, Y. Ma, P. Zhou, L. Si, and J. Chen, Chin. Opt. Lett. **10,** 021404 (2012).
3. A. S. Kurkov, Laser Phys. Lett. **4,** 93 (2007).

4. S. L. Wang, C. Y. Huang, C. C. Zhao, H. Q. Li, Y. L. Tang, N. Yang, S. Y. Zhang, Y. Hang, and J. Q. Xu, Opt. Express **21,** 17359 (2013).
5. A. S. Kurkov, V. M. Paramonov, O. I. Medvedkov, Y. N. Pyrkov, E. M. Dianov, S. E. Goncharov, and I. D. Zalevskii, Laser Phys. Lett. **3,** 151 (2006).
6. J. Faist, F. Capasso, C. Sirtori, D. L. Sivco, J. N. Baillargeon, A. L. Hutchinson, S. G. Chu, and A. Y. Cho, Appl. Phys. Lett. **68,** 3680 (1996).
7. A. S. Kurkov, V. V. Dvoyrin, and A. V. Marakulin, Opt. Lett. **35,** 490 (2010).
8. S. D. Jackson, F. Bugge, and G. Erbert, Opt. Lett. **32,** 2496 (2007).
9. S. D. Jackson, Nat. Photon. **6,** 423 (2012).
10. B. Wu, T. Chen, J. Wang, P. Jiang, D. Yang, and Y. Shen, Chin. Opt. Lett. **11,** 081901 (2013).
11. J. Wang, L. Zhang, J. Zhou, L. Si, J. Chen, and Y. Feng, Chin. Opt. Lett. **10,** 021406 (2012).
12. S. Sinha, C. Langrock, M. J. F. Digonnet, M. M. Fejer, and R. L. Byer, Opt. Lett. **31,** 347 (2006).
13. P. Zhou, X. Wang, H. Xiao, Y. Ma, and J. Chen, Laser Phys. **22,** 823 (2012).
14. A. S. Kurkov, V. M. Paramonov, and O. I. Medvedkov, Laser Phys. Lett. **3,** 503 (2006).
15. V. V. Dvoyrin, V. M. Mashinsky, O. I. Medvedkov, and E. M. Dianov, in *Proceedings of Conference on Lasers and Electro-Optics/Quantum Electronics Laser Science Conference* CWB5 (2008).
16. M. Jacquemet, A. Mugnier, G. L. Corre, E. Goyat, and D. Pureur, IEEE J. Sel. Top. Quant. Electron. **15,** 120 (2009).
17. V. V. Dvoyrin, O. I. Medvedkov, and I. T. Sorokina, IEEE J. Quant. Electron. **49,** 419 (2013).
18. I. Kelson and A. Hardy, IEEE J. Quant. Electron. **34,** 1570 (1998).
19. I. Kelson and A. Hardy, IEEE J. Lightwave Technol. Lett. **17,** 891 (1999).
20. H. Zhang, H. Xiao, P. Zhou, K. Zhang, X. Wang, and X. Xu, Appl. Phys. Express **7,** 052701 (2014).
21. J. Nilsson, J. D. Minelly, R. Paschotta, A. C. Tropper, and D. C. Hanna, Opt. Lett. **23,** 355 (1998).